

RAPID AND SENSITIVE SPECTROPHOTOMETRY METHOD BASED ON GOLD NANOPARTICLES FOR TRACE DETERMINATION OF BENZOTRIAZOLE IN AQUEOUS SOLUTIONS **

N. Esmaili, M. R. Sohrabi*, F. Motiee

Islamic Azad University, Department of Chemistry,
North Tehran Branch, Tehran, Iran; e-mail: sohrabi.m46@yahoo.co

An innovative approach was developed to determine benzotriazole (BTA) in aqueous solutions. This method was based on surface plasmon resonance (SPR) property of gold nanoparticles (AuNPs). The reaction between gold nanoparticles and benzotriazole was occurred. Then, benzotriazole was determined by spectrophotometry. Also, transmission electron microscopy (TEM) was used to show aggregation of gold nanoparticles in the presence of BTA. The effect of various parameters such as pH, contact time, concentration of gold nanoparticles, amount of buffer, and different surfactant was investigated. The proposed method is capable of determining BTA in the range of 10–100 µg/L with a limit of detection (LOD) 5 µg/L and limit of quantification (LOQ) 16 µg/L. In addition, the relative standard deviation (RSD) of this method was 2.5 and 1%. Also, benzotriazole was measured in real water samples.

Keywords: benzotriazole, gold nanoparticles, spectrophotometry, real water samples.

СПЕКТРОФОТОМЕТРИЧЕСКИЙ МЕТОД ОПРЕДЕЛЕНИЯ СЛЕДОВ БЕНЗОТРИАЗОЛА В ВОДНЫХ РАСТВОРАХ С ИСПОЛЬЗОВАНИЕМ НАНОЧАСТИЦ ЗОЛОТА

N. Esmaili, M. R. Sohrabi*, F. Motiee

УДК 543.42.062;620.3

Исламский университет Азад, Тегеран, Иран; e-mail: sohrabi.m46@yahoo.co

(Поступила 11 февраля 2019)

Разработан инновационный подход к определению бензотриазола в водных растворах. Метод основан на явлении поверхностного плазмонного резонанса на наночастицах золота. Сначала происходит реакция между наночастицами золота и бензотриазолом. Затем содержание бензотриазола определяется спектрофотометрическим методом. С помощью просвечивающей электронной микроскопии показано, что в присутствии бензотриазола происходит агрегация наночастиц золота. Исследовано влияние различных параметров, таких как pH, время контакта, концентрация наночастиц золота, количество буфера и поверхностно-активных веществ, на результат измерения бензотриазола. Предложенный способ позволяет определять содержание бензотриазола в диапазоне концентраций 10–100 мкг/л с пределом обнаружения 5 мкг/л и пределом количественного определения 16 мкг/л. Относительное стандартное отклонение метода 2.5 и 1%. Предлагаемый метод применен для измерения содержания бензотриазола в реальных образцах воды.

Ключевые слова: бензотриазол, наночастицы золота, спектрофотометрия, реальные пробы воды.

Introduction. Benzotriazole (BTA) is a high-production-volume chemical that has applications in both industrial and household [1, 2]. BTA is a heterocycle that has two fused rings and three nitrogen atoms. Its structure is shown in Fig. 1 [3]. BTA is used as electrolyte additive [4], antifungal agents [5], deicing fluid [6], medicinal chemistry [7, 8], as well as corrosion inhibitors [9, 10]. BTA is widely distributed in sur-

** Full text is published in JAS V. 87, No. 2 (<http://springer.com/journal/10812>) and in electronic version of ZhPS V. 87, No. 2 (http://www.elibrary.ru/title_about.asp?id=7318; sales@elibrary.ru).

face water such as rivers and lakes. The presence of BTA has been reported in sediment and sewage sludge [11], surface water [12], and groundwater [13]. Concentration levels from 0.1 to 6 $\mu\text{g/L}$ are environmental pollutants. Measurement of BTA is important because even low concentrations of BTA, have negative effects on aquatic organisms and human health [14, 15]. Several methods have been reported for determination of BTA, including liquid chromatography–high resolution mass spectrometry method [16], solid phase microextraction–gas chromatography–triple quadrupole mass spectrometry (SPME–GC–QqQMS) [17], chromatographic methods [18], gas chromatography–mass spectrometry (GC–MS) [19], gas chromatography (GC) with quadrupole time-of-flight mass spectrometry (QTOF–MS) [20], gas chromatography–tandem mass spectrometry (GC–MS/MS) [21], air-assisted liquid–liquid microextraction coupled with high-performance liquid chromatography [22], and so on. These methods are time-consuming, expensive, and polluting. Therefore, other methods, such as spectrophotometric methods, can be used for this purpose. Spectrophotometric methods have many advantages, including instrument availability, ease of operation, low cost, speed, precision, and accuracy. In this study, gold nanoparticles (AuNPs) were synthesized, and transmission electron microscopy (TEM) was used to characterize AuNPs. Surface plasmon resonance (SPR) is one of the interesting characterizations of AuNPs that shows a special optical behavior. This property converts the red color of AuNPs solutions to blue after the aggregate of nanoparticles [23]. Surface plasmons are quanta of plasma; a surface electromagnetic wave is a wave whose propagation is limited to the metal–dielectric interface. The surface plasmon can be stimulated by the evanescent wave, and this phenomenon is called SPR [24]. In this research, an ultraviolet–visible spectroscopy (UV–Vis) method was used based on AuNPs for determination of trace BTA in aqueous solution. The aim of this study is to show that the detection sensitivity can be significantly improved to $\mu\text{g/L}$ level by monitoring the signal changes of high UV–Vis by AuNPs. This method uses spectrophotometry techniques and does not require extraction. It is inexpensive, simple, and safe.

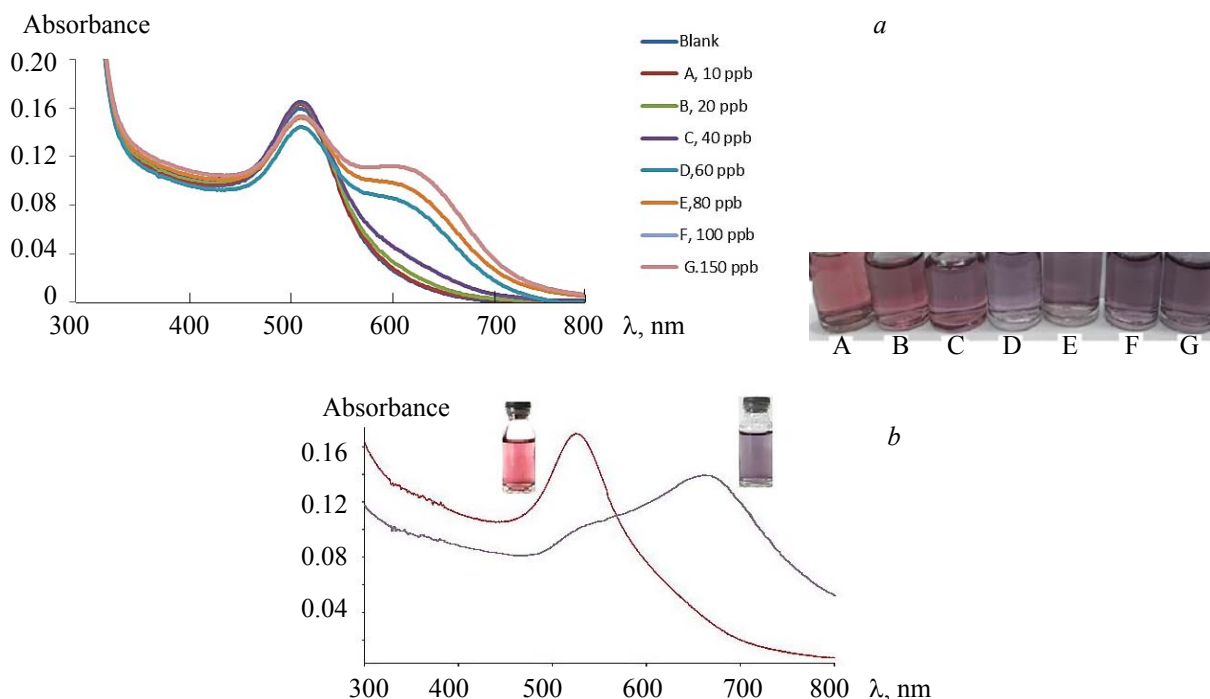


Fig. 1. (a) Overlaid UV–Vis spectra of AuNPs–BTA from 10–150 ng/mL with color changes (A–G), (b) UV–Vis spectra of AuNPs in the absence (red) and presence of BTA (blue).

Experimental. *Apparatus.* A UV–Vis spectrophotometer (Genesys 10s, American) equipped with 1.0 cm quartz cells was used for spectrophotometric measurements. A pH meter was utilized to adjust the pH values of the solutions (Inolab wtw720, Germany). The characterization of the nanoparticles was analyzed by TEM (Zeiss-EM10C-100 kV, Germany).

Materials and reagents. Benzotriazole with purity 95%, Acetone 99%, tetrachloroauric(III) acid trihydrate ($\text{HAuCl}_4 \cdot 3\text{H}_2\text{O}$) 99.5%, trisodium citrate dihydrate 99%, oxalic acid 99%, nitric acid 65%, sodium hydroxide 99%, zinc sulfate heptahydrate ($\text{ZnSO}_4 \cdot 7\text{H}_2\text{O}$), silver nitrate (AgNO_3), copper(II) sulfate pentahydrate ($\text{CuSO}_4 \cdot 5\text{H}_2\text{O}$), mercury(II) nitrate ($\text{Hg}(\text{NO}_3)_2$), manganese(II) chloride (MnCl_2), ammonium chloride (NH_4Cl), calcium carbonate (CaCO_3), ferric chloride hexahydrate ($\text{FeCl}_3 \cdot 6\text{H}_2\text{O}$), and ferrous sulfate heptahydrate ($\text{FeSO}_4 \cdot 7\text{H}_2\text{O}$) were purchased from Merck (Darmstadt, Germany). Also, double distilled water was used.

Preparation of benzotriazole solution. A stock solution of 1000 mg/L of BTA was prepared by dissolving 0.100 g of the BTA in acetone and diluting to 100 mL in a volumetric flask.

Preparation of tetrachloroauric acid solution. 0.01 g of tetrachloroauric(III) acid trihydrate was dissolved in distilled water and adjusted to the mark in a 100 mL volumetric flask. This solution was used to prepare gold nanoparticles.

Citrate solution. 1 g of trisodium citrate dehydrate was dissolved in a 100 ml volumetric flask.

Synthesis of gold nanoparticles. Trisodium citrate was used as reducing agent; 100 ml of the tetrachloroauric acid solution was heated. Then 3 ml of citrate solution was added to the stirring solution rapidly. Color changes were observed after 5 min. First, a gray solution was obtained, then purple, and eventually red. After the red color appeared, stirring and heating of the solution continued for 3 min. Then the solution was cooled at room temperature [23]. The preparation procedure is schematically shown in Fig. 1a. In addition, Fig. 1b shows the sample and control absorption spectra, the maximum wavelengths are in the region of 520 and 650 nm. By adding BTA, the absorption was transferred from 520 to 650.

Preparation and spectrophotometry analysis procedure of the test solution. 1 mL of prepared AuNPs solution (50 μM), 1 mL of oxalate buffer (pH 3.5) and different concentrations of BTA were added to 10 mL volumetric flasks and the whole diluted with double distilled water. Then, the solution was stirred. After that, a portion of this solution was transferred to a 1 cm spectrophotometer cell to record the absorbance spectrum. The same procedure was applied to the blank solution without the presence of BTA.

Preparation of real sample. Ramin power plant cooling water and drinking water of Ahwaz city were selected as real samples. The samples were kept in the refrigerator for 24 h. Then the water samples were filtered by filter paper to remove suspended particles. BTA was added to a final concentration of 5 and 20 $\mu\text{g/L}$. Different concentrations of BTA were spiked into each water sample (every 100 ml). Then 0.2 ml oxalate buffer (pH 3.5) and 1 ml of AuNPs solution (50 μM) were added and the whole stirred. Finally, the BTA content of each sample was determined at optimum conditions by a spectrophotometer.

Results and discussion. TEM analysis. Figure 2 presents the TEM image of the AuNPs, which identifies an average size of 18 nm. This effect was related to the interaction between nitrogen atoms of BTA and gold.

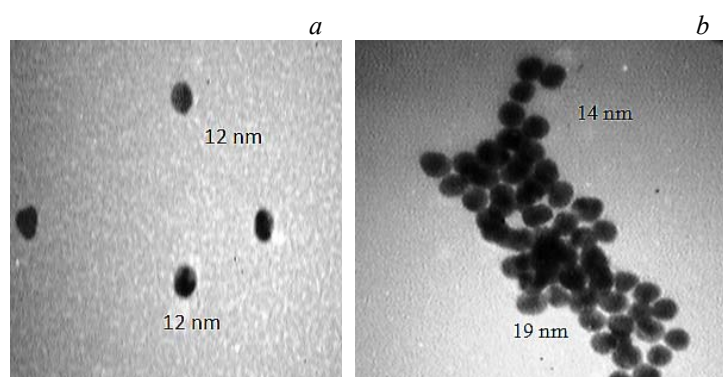


Fig. 2. TEM images of AuNPs (a) before and (b) after adding BTA.

Optimization. The effect of pH on the absorbance of the system over the range of 2.5–9 was investigated. As shown in Fig 3a, the maximum pH is 3.5 in a volume of 10 mL at a concentration of AuNPs of 50 $\mu\text{mol/L}$ and a concentration of BTA of 100 ng/mL.

AuNPs are negatively charged particles. Therefore, the reaction between AuNPs and BTA occurs at a reduced pH due to AuNPs neutralization [25]. Also, three buffers, including phthalate, formate, and oxalate, were investigated to choose the suitable buffer. For this purpose, the oxalate buffer proved to be the best buffer; 1.0 mL of oxalate buffer was selected as optimum. The results are shown in Fig 3b.

Due to the undeniable significance of AuNPs concentration and the role of it in this method, different concentrations of AuNPs were used to study the absorption spectra. Figure 3c shows that there is a positive correlation with increasing amounts of AuNPs due to A_{650}/A_{520} ratio. Therefore, the optimum concentration of AuNPs was 50 μM .

In addition, the effect of surfactant concentrations on the measurement of BTA was studied in 10 ml of 20 $\mu\text{g/L}$ solution BTA. At this stage, TX100 (neutral surfactant), CTAB (cationic surfactant) and SDS (anionic surfactant) were used. The results are shown in Fig. 3d. The presence of surfactant created an aggregation phenomenon, which reduced the absorption of nanoparticles. The results show that in the presence of cationic surfactants such as CTAB, absorption can be reduced in AuNPs and nanoparticles with BTA. Also, anionic surfactants were studied, and it was observed that the intensity of absorbance for both solutions was significantly reduced. Based on these results, it can be seen that the highest absorption and sensitivity were obtained in the absence of surfactant.

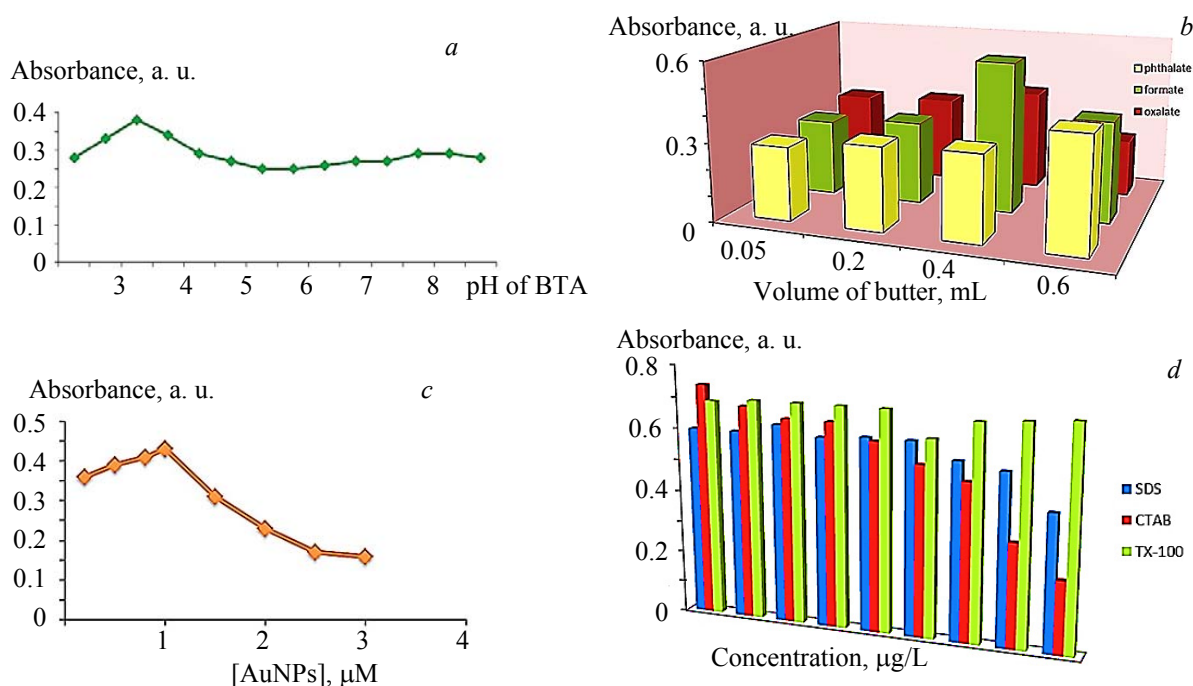


Fig. 3. Effect of (a) pH, (b) buffer, (c) change in the concentration of AuNPs, and (d) surfactant concentration on the surface plasmon intensity.

Furthermore, the effect of interaction time on absorption spectra was investigated in the range of 1–20 min. In all the cases, the absorption spectra did not change dramatically and fall in a straight line. This means that the interaction between BTA and AuNPs does not require time and is fast.

Interference studies. Under the experimental conditions, a number of cations and anions including Cu^{2+} , Mn^{2+} , NH_4^+ , SO_3^{2-} , Hg^{2+} , Ag^+ , Fe^{2+} , Pd^{2+} , Ca^{2+} , Al^{3+} , and Zn^{2+} were investigated for the interference effect on the determination of 100 $\mu\text{g/L}$ of BTA. The tolerance limit was defined as the maximum concentration of potentially interfering ions that cause $\pm 5\%$ error in the determination of BTA. Table 1 shows that the developed method is relatively selective for the determination of BTA. Also, the results indicated that the involved ionic species had no significant, measurable impact.

TABLE 1. Effect of Different Interference Species on the Measurement of BTA

X = Specified species	Concentration of interfering ion, $\mu\text{g/L}$	Tolerance limits $[X]/\text{BTA}$
Cu^{2+} , Mn^{2+} , NH_4^+ , SO_3^{2-}	100	1000
Hg^{2+}	5	50
Ag^+ , Fe^{2+} , Pd^{2+}	2	20
Ca^{2+} , Al^{3+} , Zn^{2+}	1	10

Calibration graphs and detection limits. Under precisely controlled conditions, the calibration graph was obtained by plotting absorbance values versus the BTA concentration. The calibration graph showed good linearity in the range of 10–150 ng/mL with correlation coefficient $R^2 = 0.9941$ as shown in Fig 4. The limit of detection (LOD) is the analyte concentration producing a signal equal to the blank signal, y_B , plus three standard deviations of the blank signal, s_B [26]:

$$\text{LOD} = y_B + 3s_B. \tag{1}$$

It was found to be 5 $\mu\text{g/L}$. The precision of the method was evaluated by performing eight repeated measurements of solutions containing 40 and 120 $\mu\text{g/L}$ of BTA. Furthermore, the relative standard deviations (RSD) for these determinations were 2.5 and 1%, respectively.

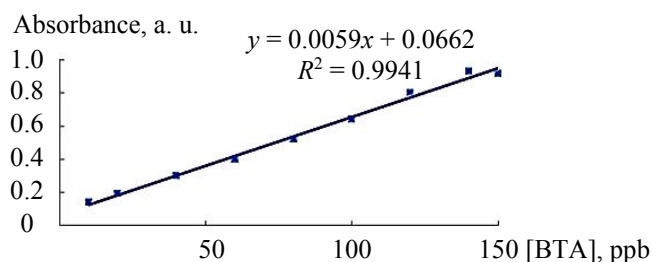


Fig. 4. Calibration curve for determination of BTA from 10–150 ng/mL.

Determination of BTA in water samples. In order to verify the proposed method, the developed procedure was applied for determination of BTA in real water samples. Recovery tests were used to assay the reliability and accuracy of the method. The BTA content of different water samples and recoveries of added analytes were evaluated. The results are summarized in Table 2, which shows that it was possible to determine the BTA concentration in real sample solutions using the proposed method outlined in this investigation. Recovery was calculated using the following formula [27]:

$$\text{Recovery (\%)} = \text{Measured/Expected} \times 100.$$

Comparison with the other methods. The proposed method was compared with the other methods, and the results are summarized in Table 3. The results indicate that the accuracy of the proposed method is satisfactory. Also, LOD and RSD of this method are close to or better than the previous reported methods.

TABLE 2. Analytical Results of Measurement by the Proposed Method ($n = 5$) in Water Samples

Sample	BTA added, $\mu\text{g/L}$	BTA found ^a , $\mu\text{g/L}$	Recovery, %
Ahwaz drinking water	–	5.9±0.05	
	5	10.5±0.06	92.00
	20	25±0.06	95.50
Ramin power plant cooling water	-	63.5±0.09	
	5	68.3±0.06	96.00
	20	82.2±0.07	93.50

^aMean ± standard deviation.

TABLE 3. Comparison of Several Methods for Determination of BTA

No.	Method	Linear range, ng/mL	LOD, ng/mL	RSD, %	Real sample	References
1	SPE ^a	–	0.001–0.1	<15	river water and sewage	[28]
2	Extraction	500–10000	–	6	soil samples	[29]
3	SPME ^b	2.5–100	2	6.0–0.6	tap water	[17]
4	Spectrophotometry	1–150	5	2.5 (40) 1(120)	drinking water and industrial water	Present study

^a Solid phase extraction.

^b Solid-phase microextraction.

Conclusions. This study can be summarized as follows. A new optical method for the sensitive spectrophotometry detection of BTA based on surface plasmon resonance absorption peak of AuNPs was developed. Stable and dispersed AuNPs were applied using a simple, rapid, and environmentally-friendly procedure by applying citrate. In the presence of BTA, plasmon intensity of AuNPs decreases (the absorbance change at λ_{max} , 650 nm, was used for determination of BTA). The proposed method is easier and more cost effective than existing methods for the measurement of low amounts of BTA. Thus, this method can be used for the determination of BTA in the range of 10–150 $\mu\text{g/L}$ with a limit of detection 5 $\mu\text{g/L}$ in both industrial and drinking water. Important factors such as pH, contact time, concentration of AuNPs, role of surfactants, and ionic species contribution were evaluated. None had a significant and measurable impact.

REFERENCES

1. E. Jover, V. Matamoros, J. Maria Bayona, *J. Chromatogr., A*, **1216**, 4013–4019 (2009).
2. Y. S. Liu, G.G. Ying, A. Shareef, R. S. Kookan, *Environ. Pollut.*, **165**, 225–232 (2012).
3. Y. Li, J. Wang, W. Guo, C. Gao, Z. Cheng, *Instrum. Sci. Technol.*, **45**, 290–300 (2017).
4. L. Hamenu, A. Madzvamuse, L. Mohammed, *J. Ind. Eng. Chem.*, **53**, 241–246 (2017).
5. M. Lv, J. Ma, Q. Li, Hui Xu, *Bioorg. Med. Chem. Lett.*, **28**, 181–187 (2018).
6. G. D. Breedveld, R. Roseth, M. Sparrevik, T. Hartnlk, L. J. Hem, *Water, Air, Soil Pollut.*, **3**, 91–101 (2003).
7. G. K. Patil, H. C. Patil, I. M. Patil, S. L. Borse, S. P. Pawar, *World J. Pharm. Pharm. Sci.*, **4**, 532–548 (2015).
8. N. P. Milosevic, V. B. Dimova, N. U. Perisic-Janjic, *Eur. J. Pharm. Sci.*, **49**, 10–17 (2013).
9. M. M. Mennucci, E. P. Banczek, P. R. P. Rodrigues, I. Costa, *Cement Concrete Compos.*, **31**, 418–424 (2009).
10. K. Wang, H. W. Pickering, K. G. Weil, *J. Electrochem. Soc.*, **150**, B176–B180 (2003).
11. Z. Zhang, N. Ren, Y.F. Li, T. Kunisue, D. Gao, K. Kannan, *Environ. Sci. Technol.*, **45**, 3909–3916 (2011).
12. W. Giger, C. Schaffner, H. P. Kohler, *Environ. Sci. Technol.*, **40**, 7186–7192 (2006).
13. R. Loos, G. Locoro, S. Comero, S. Contini, D. Schwesig, F. Werres, P. Balsaa, O. Gans, S. Weiss, L. Blaha, M. Bolchi, B. Manfred Gawlik, *Water Res.*, **44**, 4115–4126 (2010).
14. C. Dominguez, C. Reyes-Contreras, J. M. Bayona, *J. Chromatogr., A*, **1230**, 117–122 (2012).
15. N. Haji Seyed Javadi, M. Baghdadi, N. Mehrdadi, M. Mortazavi, *J. Environ. Chem. Eng.*, **6**, 6421–6430 (2018).
16. P. Herrero, F. Borrull, R. M. Marce, E. Pocurull, *J. Chromatogr., A*, **1355**, 53–60 (2014).
17. A. Naccarato, E. Gionfriddo, G. Sindona, A. Tagarelli, *J. Chromatogr., A*, **1338**, 164–173 (2014).
18. E. Patsalides, K. Robards, *J. Chromatogr.*, **331**, 149–160 (1985).
19. W. Xu, W. Yan, T. Licha, *J. Chromatogr., A*, **1422**, 270–276 (2015).
20. J. Casado, I. Rodriguez, I. Carpinteiro, M. Ramil, R. Cela, *J. Chromatogr., A*, **1293**, 126–132 (2013).
21. Y. S. Liu, G. G. Ying, A. Shareef, R. S. Kookana, *J. Chromatogr., A*, **1218**, 5328–5335 (2011).
22. L. Jing, W. Meng-Meng, W. Qiang, L. Hai-Pu, Y. Zhao-Guang, *Chin. J. Anal. Chem.*, **46**, 1817–1824 (2018).
23. R. Asrariyan, S. Elhami, *Chem. Pap.*, **71**, 2301–2308 (2017).
24. Y. Tang, X. Zeng, *J. Chem. Ed.*, **87**, 742–746 (2010).
25. H. Parham, N. Pourreza, F. Marahel, *Spectrochim. Acta, Mol. Biomol. Spectrosc.*, **151**, 308–314 (2015).
26. J. N. Miller, J. C. Miller, *Statistics and Chemometrics for Analytical Chemistry*, 6th ed., ISBN-978-0-273-73042-2 (2010).
27. A. A. Szalay, P. J. Hill, L. J. Kricka, *Bioluminescence and Chemiluminescence: Chemistry, Biology and Applications*, 1st ed., World Scientific Publ. (2007).
28. P. Herrero, F. Borrull, E. Pocurull, R. M. Marce, *J. Chromatogr. A*, **1309** (2013) 22–32.
29. A. Speltini, M. Sturini, F. Maraschi, A. Porta, A. Profumo, *Talanta*, **147** (2016) 322–327.